The Korean Journal of Ceramics, **2** [1] 25-32 (1996)

Synthesis of Solid Electrolyte Nasicon by Solid State Reaction

Cheol-Jin Kim, Jun-Ki Chung, Sung-Ki Lim* and Meung-Ho Rhee**

Dept. of Inorg. Mater. Eng. and Advanced Materials Research Institute, Gyeongsang National Univ., Gajwa-dong 900, Chinju 660-701, Korea
**Dept. of Industrial Chemistry, KonKuk Univ., Mojin-dong 93-1, Kwangjin-ku, Seoul 133-701, Korea*
***Korea Automotive Technology Institute, Yongjeong-Lee, Pungse-myun, Chungnam 330-910, Korea*
(Received January 26, 1996)

Solid electrolyte nasicon was synthesized by the optimized solid state reaction minimizing the volume fraction of secondary ZrO_2 and glassy phases. To compensate for the evaporation of Na and P during heat-treatment, excess Na and P were added to the starting composition $Na_{1+x}Zr_2Si_xP_{3-x}O_{12}$ (x=2.1). Phase pure nasicon comparable in volume fraction to the one obtained from sol-gel process were synthesized after the reaction at 1100~1150°C, P_{O2}= 0.1-0.15 atm for 24 hrs. The volume fraction of ZrO_2 increased with the heat-treatment time due to the decomposition of nasicon phase and that of glassy phase increased as partial oxygen pressure decreased. The synthesized nasicon showed a good electrical conductivity of $\sim 1\times10^{-2}(\Omega\cdot cm)^{-1}$ at 350°C.

Key words : NASICON, ZrO_2 second phase, Solid-state sintering, Atmosphere control

I. Introduction

β''-Al_2O_3 and nasicon (Na SuperIonic CONductor) are typical materials among the solid electrolytes with high Na^+ ion conductance, which are called super-ionic conductor, hyper-ionic conductor, or fast-ionic conductor and can be applied to gas sensor, high-temperature fuel cell, separator material for energy storage batteries.[1-4] Na^+ β-alumina has 2 polymorph of hexagonal β-Al_2O_3 and rhombohedral β"-Al_2O_3. Although β"-Al_2O_3 has high ionic conductance, it has some shortcomings such as 2-dimensional ionic conduction mechanism due to its layered structure, low resistance against the moisture, and high sintering temperature above 1500°C. High sintering temperature not only increases the production cost but also makes the composition control difficult due to the Na evaporation during the heat treatment.

Nasicon, which has composition range of $Na_{1+x}Zr_2Si_xP_{3-x}O_{12}$ ($0\leq x\leq 3$) or $Na_{1+x+4y}Zr_{2-y}Si_xP_{3-x}O_{12}$ ($0\leq x\leq 3$, $x+3y\leq 3$),[5,6] is a solid solution between $NaZr_2P_3O_{12}$ (rhombohedral structure) and $Na_4Zr_2Si_3O_{12}$ (monoclinic structure). Nasicon has higher resistance against moisture compared to β"-Al_2O_3, 3-dimensional conduction path along the 3-dimensionally connected Na^+ ion site in the framework structure, and high energy density. Therefore, nasicon has a practical potential over β"-Al_2O_3 if several processing problems are overcome. Nasicon with the composition of $1.8\leq x\leq 2.2$ has high ionic conductivity of 0.1~$0.2\Omega^{-1}cm^{-1}$ at 300°C, the working temperature of Na/S battery. Although this high conductivity is comparable to β"-Al_2O_3, nasicon undergoes phase transition between the rhombohedral structure (high temperature form) and monoclinic structure (low temperature form) in the temperature range of 150~300°C.[7-8] The electrical, mechanical, chemical, and anisotropic properties of the nasicon single crystal undergoes changes during the phase transition and the mechanical strength also deteriorates at working temperature, all of which act as obstacles to the practical use of nasicon.[9] Incomplete reaction of the starting materials, Na evaporation during the sintering, and the decomposition of nasicon bring about the free ZrO_2 phase in the matrix, which greatly reduces the life cycle of the device by introducing micro-cracks during operation.[10] Therefore, it is necessary to synthesize the sintered body of phase-pure nasicon, which fundamentally require sintering temperature above 1200°C. The vapor pressure of Na and P above 1200°C is large enough that a portion of Na and P in the starting composition evaporate, resulting in the formation of free ZrO_2. Also using a ZrO_2-deficient starting composition to avoid the free ZrO_2 formation results in glassy phase in the grain boundaries.

Sol-gel process among the many works[10,11] to avoid the formation of free ZrO_2 has been reported successful to obtain almost single-phase nasicon,[11] but its practical application to the mass production such as for the device of the electric vehicle is inappropriate, since the production cost is relatively higher than that of solid state reaction. In this study, conditions of solid state reaction including starting composition, sintering temperature, heat treatment time, and atmosphere have been explored to synthesize a phase-pure nasicon comparable to the one obtained by sol-gel process by minimizing the volume fraction of free-ZrO_2 and glassy phase during the sintering process. Among the various problems associated with the nasicon synthesis such as phase transition with tem-

perature and compositional variation, we have focussed on the condition reducing the volume fraction of free-ZrO_2 and increasing the volume fraction of nasicon during the solid state reaction in this study.

II. Experimental

The formation mechanism of nasicon was reported by V.A. Nicholas *et al.*[7] as a peritectic reaction where Zr diffuses into Na-Si-P-O intermediate compound, and recently phase diagram in the quarternary system Na_2O-SiO_2-ZrO_2-P_2O_5 has been reported.[12] Since it is difficult to control the precise reaction paths due to the sluggish peritectic reaction, we have tried to synthesize the phase-pure nasicon by optimizing the starting materials and composition, heat-treatment conditions(temperature, time, atmosphere), and compensation for the Na and P evaporation (Fig. 1). DTA analyses were conducted to follow the thermal events of the starting materials using DAT/TG (Rigaku, Thermoflex model). Phases present in the sintered samples were identified by X-ray diffraction (XRD, Rigaku, D/Max X-ray diffractometer, 1.8 kW) using Cu K_α radiation and Ni filter. Microstructure and chemical composition were analyzed using scanning electron microscopes (SEM, Akashi SX-40A and JEOL JSM-6400) with an energy dispersive spectroscopy. Also electrical conductivity of the specimens which showed almost phase-pure nasicon in the XRD patterns were measured.

1. Optimization of the starting composition

Since the intermediate compounds and the final nasicon phase are affected by the starting materials, Na_2CO_3 (Aldrich, 99.5+%), Na_2HPO_4 (Aldrich, 99+%), or $(NH_4)_2HPO_4$ (Aldrich, 98%) was used as Na source, ZrO_2 (Aldrich, 99%), $ZrO(NO_3)_2 \cdot xH_2O$ (Aldrich, reagent grade), or $ZrF_4 \cdot xH_2O$ (Aldrich, 97%) was used as Zr source, selectively. Starting materials of Na_2CO_3, Na_2HPO_4, $(NH_4)_2HPO_4$, ZrO_2, $ZrO(NO_3)_2 \cdot xH_2O$, $ZrF_4 \cdot xH_2O$, SiO_2 (Aldrich, 99.8%) were weighed to make x=2.0, 2.1, 2.2 in the nasicon composition ($Na_{1+x}Zr_2Si_xP_{3-x}O_{12}$). The weighed starting materials were wet-milled in ethanol media using zirconia balls in a micro ball-mill for 24 hrs, and dried at 60~80°C while stirring using infrared lamps. The dried powder was calcined at 300°C for 2hrs and subsequently at 900°C for 6 hrs. The powder was pelletized with 20000 psi using 15 mm ϕ mold. The pellets were heat-treated at 950~1300°C for 12 hrs unit, up to 48 hrs. Since the peritectic reaction is sluggish and Zr-diffusion into the grain might not be complete, the 2nd heat-treatment was conducted after pulverizing and pelletizing the heat-treated samples with the same condition as the 1st heat-treatment to ensure the complete reaction.

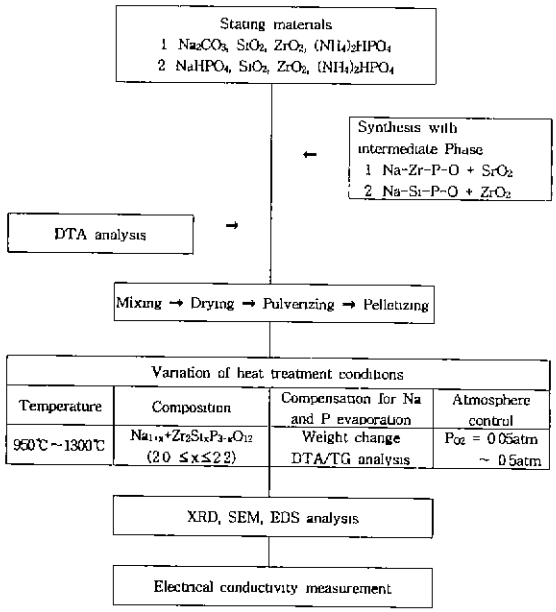

Fig. 1. Flow chart of the experimental procedure for synthesis of nasicon.

2. Variation of reaction temperature and time

To detect the formation temperature of nasicon phase, DTA/TG experiments were conducted varying the specimen weight (10 mg~20 mg) and heating rate (10°C/min, 5°C/min, 2°C/min). Distinct endothermic peak did not appear above 1000°C due to the sluggish reaction, rather baseline of the DTA curve gradually increased in the 900~1200°C range where nasicon phase was assumed to form (Fig. 2). In Fig. 2 (a), the endothermic peak below 200°C has been reported to occur due to the reaction $NH_4H_2PO_4$

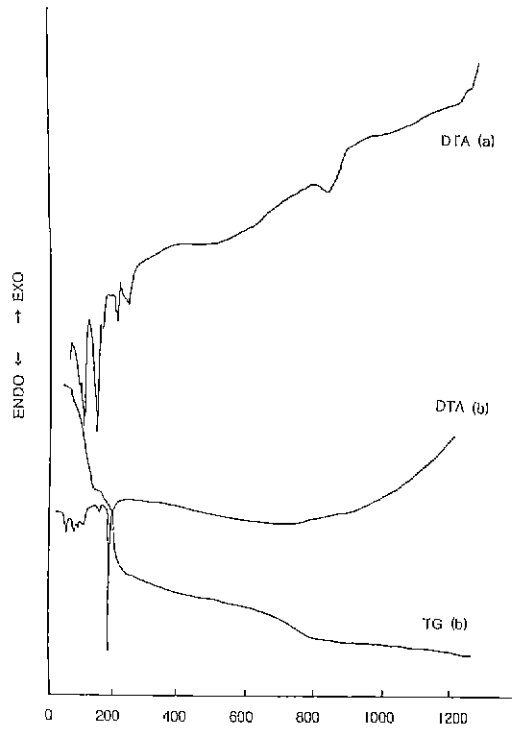

Fig. 2. DTA/TG curves of $Na_{1+x}Zr_2Si_xP_{3-x}O_{12}$ (x=2.1) with raw materials a) Na_2CO_3, $NH_4H_2PO_4$, ZrO_2, SiO_2, showing no distinct endothermic peak above 1000°C.

$\rightarrow H_3PO_4 + NH_3$ and $NH_4H_2PO_4 + Na_2CO_3 \rightarrow Na_2HPO_4 + CO_2 + H_2O$.[7] And the endothermic peak at about 850°C corresponds to the decomposition of unreacted Na_2CO_3. The endothermic peak at 195°C in Fig. 2 (b) corresponds to the decomposition of Na_2HPO_4 into $Na_4P_2O_7 + H_2O$ accompanying weight loss, and the endothermic peak at about 850°C did not appear in Fig. 2 (b) since the starting composition did not contain Na_2CO_3. It was assumed that the reaction kinetics were very slow, since there was not any detectable endothermic peak in the 900~1200°C temperature range which had been reported as reaction temperature range of nasicon phase.[7] Thus reaction temperature was divided into 25~50°C interval over 950~1300°C temperature region and reaction time was also divided into 12 hrs unit. After the reaction, degree of formation of nasicon phase was estimated by XRD intensities. In the 1050~1150°C temperature range where the volume fraction of nasicon phase is higher than the other temperature range, samples were heat-treated for 6 hrs interval to understand the degree of reaction with the time, and relative XRD intensities $\frac{I_{ZrO_2}(111)}{I_{nasicon}(020)}$ were measured. From this relative XRD intensities, the volume fractions of the nasicon in the samples after the heat-treatment was estimated.

3. Synthesis with intermediate compounds

As the cause of free ZrO_2, incomplete reaction of the starting materials, evaporation of Na and P, and the decomposition of the intermediate compounds or already formed nasicon itself can be mentioned. Among these, incomplete reaction arises from the sluggish diffusion of Zr during the peritectic reaction. When the samples are quenched from 1000°C, intermediate compounds with variable compositions and starting materials such as $Na_4Zr_2Si_2O_4$, Na_2SiO_3, or ZrO_2 have been reported to found.[12] The intermediate compounds are known to form when ZrO_2 dissolves into sodium silicate. The main reaction path of the nasicon formation is the dissolution of ZrO_2 into (Na-P-Si-O) intermediate compounds, which occurs by slow diffusion of Zr^{4+} ion, thus acts as a rate-determining step. In order to bypass the sluggish diffusion of Zr^{4+} ion to maximize the volume fraction of nasicon and minimize the quantity of free-ZrO_2, reactions using intermediate compounds were tried. There are the 2 kinds of reactions reported; 1) intermediate compound (Na-Zr-P-O) + SiO_2, 2) intermediate compound (Na-Si-P-O) + ZrO_2. The reaction 1) complete at around 1200°C and the reaction 2) complete at around 1100°C.[12]

1) $(Na_3PO_4+ZrO_2) \rightarrow$ amorphous intermediate $\rightarrow$ nasicon
$\nearrow$
SiO_2

2) $(Na_3PO_4+SiO_2) \rightarrow$ amorphous intermediate $\rightarrow$ nasicon
$\nearrow$
ZrO_2

Since the reaction 2) is sluggish and requires a high temperature ($\geq$1250°C), the amount of evaporation of Na and P may increase, accordingly the quantity of unreacted free-ZrO_2 increase. To use the reaction 1), intermediate compound with the nasicon composition except Si were prereacted at 1000~1300°C, SiO_2 were added in the later heat treatment, and then samples were analyzed with XRD.

4. Atmosphere control and compensation for the Na and P evaporation

It is necessary to compensate for the Na and P loss during the heat-treatment above 1000°C. Since evaporation of Na and P causes the incomplete reaction of nasicon formation and residual ZrO_2, excess Na and P were added approximately 2~10 wt% to the starting composition which were estimated by the weight loss except the gas phases before and after the heat treatment. The atmosphere was controlled by a proportioning rotameter (OMEGA) with O_2 and Ar gas to give the oxygen partial pressure of P_{O2}=0.05 atm, P_{O2}=0.1 atm, P_{O2}=0.15 atm, P_{O2}=0.21 atm, P_{O2}=0.5 atm, and calibrated with oxygen sensor composed of 8% Y_2O_3-ZrO_2 cell. To maintain precise oxygen partial pressure, tube furnace with the specimens were initially evacuated with a mechanical vacuum pump, and then mixed gas was slowly circulated into the tube. The microstructure and the phases in the samples after the heat treatment were analyzed again with XRD and SEM.

5. Electrical conductivity measurement

Electrical conductivity was calculated from the resistance measured with conductivity bridge (YSI model 31, AC 1 kHz). The thickness of the polished specimen was measured with vernier-calipers and Pt-paste (Johnson Matthey) was applied to the approximately 2 mm×2 mm area of the nasicon pellets (ϕ=15 mm) to form electrodes. The specimens were calcined at 900°C for 20 min. Resistance was measured in the tube furnace with kanthal heating element at 350°C and Pt and Pt-Rh (13%) were used as lead wires for the electrode. Conductivity of the nasicon was calculated by substituting the measured value for the electrode area, distance between the electrodes, and the resistance in the following equation.

$$R = \rho \frac{1}{A} = \frac{1}{k} \cdot \frac{1}{A}$$

R: electrical resistance between the electrodes (ohm)
ρ: Specific resistance of the solution measured with Wheatstone bridge
l: distance between the electrodes (cm)
A: electrode area (cm^2)
k: specific conductance

III. Results and Discussions

1. The effect of the starting composition and excess Na and P

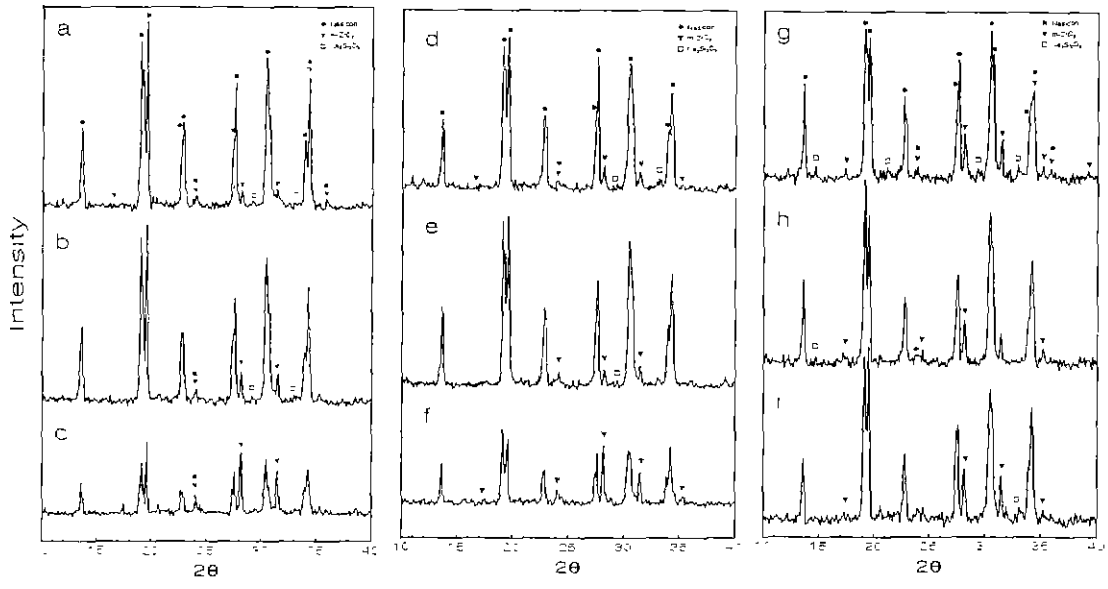

Fig. 3. XRD-patterns of NASICON, ($Na_{1+x}Zr_2Si_xP_{3-x}O_{12}$) with different starting compositions of x=2 0 (a,b,c), x=2.1 (d,e,f) and x=2. 2 (g,h,i) which were heat-treated in air for 24 hrs at 1200°C (a,d,g), 1225° (b,e,f) and 1250°C (c,f,i), respectively.

From the preliminary experiments, the composition $Na_{1+x}Zr_2Si_xP_{3-x}O_{12}$ (x=2.0, 2.1, 2.2) resulted in easy formation of nasicon phase and least amount of free ZrO_2 phase after the heat-treatment in air atmosphere. The subsequent experiments were based on these compositions. XRD peaks of ZrO_2 were observed at d=5.079Å, 3.636Å, 3.163Å, 2.839Å, but the peak with the relative intensity I/I_o=100 at d=3.163Å could be easily distinguishable from the other peaks of the sample. The relative quantity of free-ZrO_2/nasicon phase was estimated from the relative intensity $I_{ZrO_2(111)}/I_{nasicon(020)}$. All the three starting compositions showed relatively strong ZrO_2 peaks after heat-treatment in the temperature range of 1100~1250°C. The intensity of the ZrO_2 peaks increased with temperature and time, and the samples reacted at 1250°C exhibited large volume fraction of ZrO_2 regardless of the starting compositions. This tendency can be clearly shown in Fig. 3, where XRD patterns were taken from the samples with the starting composition $Na_{1+x}Zr_2Si_xP_{3-x}O_{12}$ (x=2.0, 2.1, 2.2) after the heat-treatment at 1200°C, 1225°C, 1250°C in air for 24 hrs. As the x-value in the composition increases in Fig. 3, the intensities of $Na_2Si_2O_5$ phase decreased. It could be simply thought as that the XRD intensity of $Na_2Si_2O_5$ should increased as x-value since the content of Na and S increased and the content of P decreased. But it is more plausible to think that the composition with x=2.0 in the quarternary system Na_2O-ZrO_2-SiO_2-P_2O_5 lies in the phase boundary where two phases can coexist and that the composition with x=2.2 locates within the phase boundary. Also $Na_2Si_2O_5$ phase has been reported to easily form during cooling of the partially melted nasicon.[7] The increase of the volume fraction of ZrO_2 in the SEM micrographs could not be identified quantitatively, since

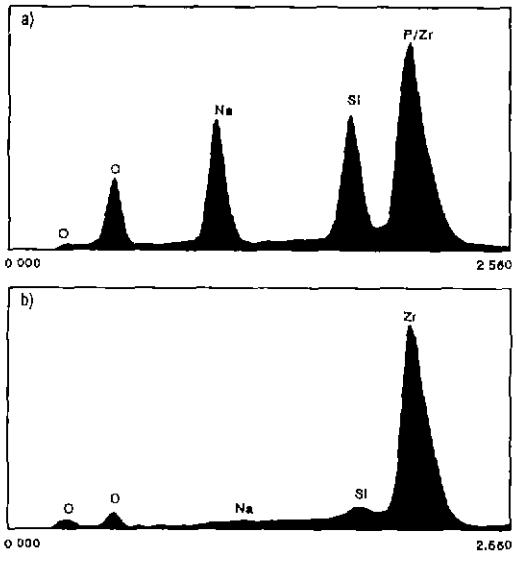

Fig. 4. EDS spectra from a) Nasicon phase region, b) free ZrO_2 aggregates.

not only the particle size was small but also the distribution was irregular. EDS analyses of the small particles smaller than 1 μm on the surface of nasicon turned out to be ZrO_2, as shown in Fig. 4. Although the peaks corresponding to Na and Si showed small intensities, they were assumed come from the matrix phase around tiny ZrO_2 particles. However, the quantitative analysis of the nasicon phase was impossible since the $K_{\alpha 1}$ peak of P (2.014 keV) and the $L_{\alpha 1}$ of Zr(2.042 keV) were overlapped.

The formation of liquid eases the diffusion of Zr^{4+} ion which is crucial for the formation of nasicon. Liquid phase during the heat treatment can be easily formed as higher the reaction temperature, or lower the oxygen par-

tial pressure, or higher the content of Na and P in the starting composition which accelerate formation of compounds with low melting temperatures. All these experimental variables accelerate the formation of $Na_2Si_2O_5$ phase, resulting in the formation of glassy phase around the nasicon grain during cooling. Therefore, it was necessary to combine the experimental parameters to obtain the optimized effect on the electrical conductance.

Since the possibility of the evaporation of Na and P from the surface of the sample is greater than from the inside of the sample, the samples were covered with the powder of the same composition as the sample itself. By adding excess Na and P to make the starting composition $Na_{3.4}Zr_2Si_{2.1}P_{1.2}O_{12}$, the quantity of free ZrO_2 greatly decreased after the heat treatment. Covering the specimen with the powders of starting composition did not show any noticeable difference in the XRD peak intensities from the uncovered one. Also the grain size of the nasicon was observed to increase as with the introduction of excess Na and P. Single crystalline nasicon phase smaller than 1 μm and with almost cubic morphology were observed in the sample with the composition x=2.1 in the SEM micrograph (Fig. 5).

2. *The effect of the partial oxygen pressure P_{O2}*

As the P_{O2} decreases, liquid phase is easily formed, accelerating the diffusion of Zr^{4+} ion which is rate-determining step for the formation of nasicon, and reducing the free-ZrO_2 volume fraction. The effect of the partial oxygen pressure on the formation of nasicon was not yet clearly reported. In this study, heat treatment was conducted at P_{O2}=0.05, 0.10, 0.15, 0.21, 0.5 atm, and at T= 1100°C and 1150°C, expecting the promotion of Zr^{4+} diffusion rate. Most of the experiments were conducted in the reducing atmosphere, since the melting temperature of nasicon increased in oxydizing atmosphere. Fig. 6 shows the SEM microstructure of the samples with the composition x=2.1 and x=2.2 in the $Na_{1+x}Zr_2Si_xP_{3-x}O_{12}$, heat treated twice for 12 hrs at P_{O2}=0.05 atm, 0.10 atm, 0.15 atm. All the microsgraphs look similar, showing nasicon grains, glassy phase around the nasicon phase, and many pores. The sample with x=2.2 composition showed slightly more glassy phase than x=2.1 composition. This indicate that the quantity of liquid phase increased at lower P_{O2} as we expected and liquid phase turned into glassy phase or $Na_2Si_2O_5$ during cooling stage. Although the difference of XRD patterns as with P_{O2} was not large enough, the XRD intensities of ZrO_2 peaks were smallest in the sample at P_{O2}=0.10 atm and 0.15 atm. Also the samples heat treated at 1100°C showed better developed nasicon phase than that at 1000°C (Fig. 7).

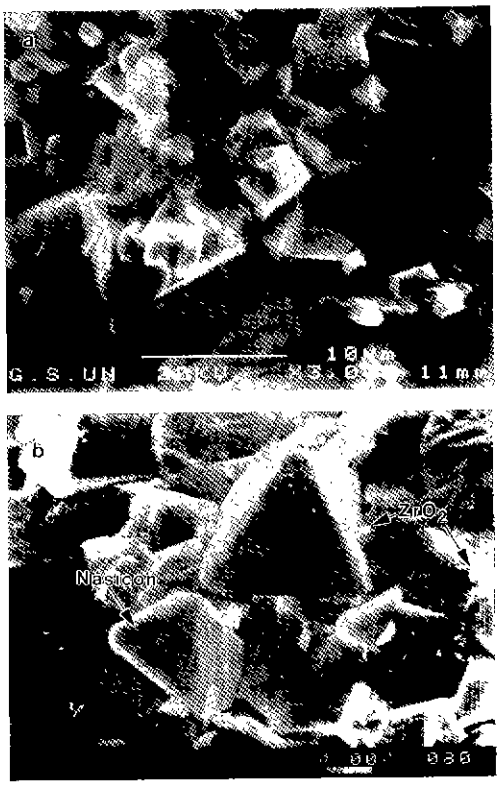

Fig. 5. SEM micrographs of the Na/P enriched Nasicon ($Na_{3.4}Zr_2Si_{2.1}P_{1.2}O_{12}$) heat-treated at 1100°C for 24 hrs. showing a) the cube-like Nasicon phase, and b) another area with the tiny ZrO_2 phase.

3. *The effect of the compensation for the Na and P loss*

Since the formation temperature of nasicon phase is above 1000°C, the vapor pressure of Na and P is high enough to evaporate, causing the incomplete reaction of nasicon due to the deficiency of Na and P. The amount of Na and P evaporation were measured respectively by simple weight comparison before and after the heat treatment in the ternary system Na_2CO_3-SiO_2-ZrO_2 and $(NH_4)_2HPO_4$-SiO_2-ZrO_2. Approximately 2 wt% of Na-loss was detected, but P-loss could not be measured in the simple weight comparison. DTA/TG experiment holding temperature at 1000°C for 12 hrs showed more weight loss than 2 wt%, which means there occurred P-loss. Therefore, approximately 2~10 wt% of excess Na and P were added to the starting composition gradually since the exact amount of the loss during the heat-treatment could not be measured. Fig. 8 shows the XRD patterns of the samples with x=2.1 which were heat-treated at 1150 and at P_{O2}=0.05, 0.10, 0.15, 0.21 atm. It also shows that the effect of P_{O2} and the temperature overwhelmed the effect of covering the samples with the powders of the same compositions.

The evaporation of Na and P is greater in the process using intermediate compounds for the nasicon synthesis, since the reaction temperature of the intermediate phase is 1300°C, much higher than the reaction temperature of nasicon in this study. Large amount of ZrO_2 existed in the samples derived from the intermediate compound at 1200°C, and could not be eliminated by simply in-

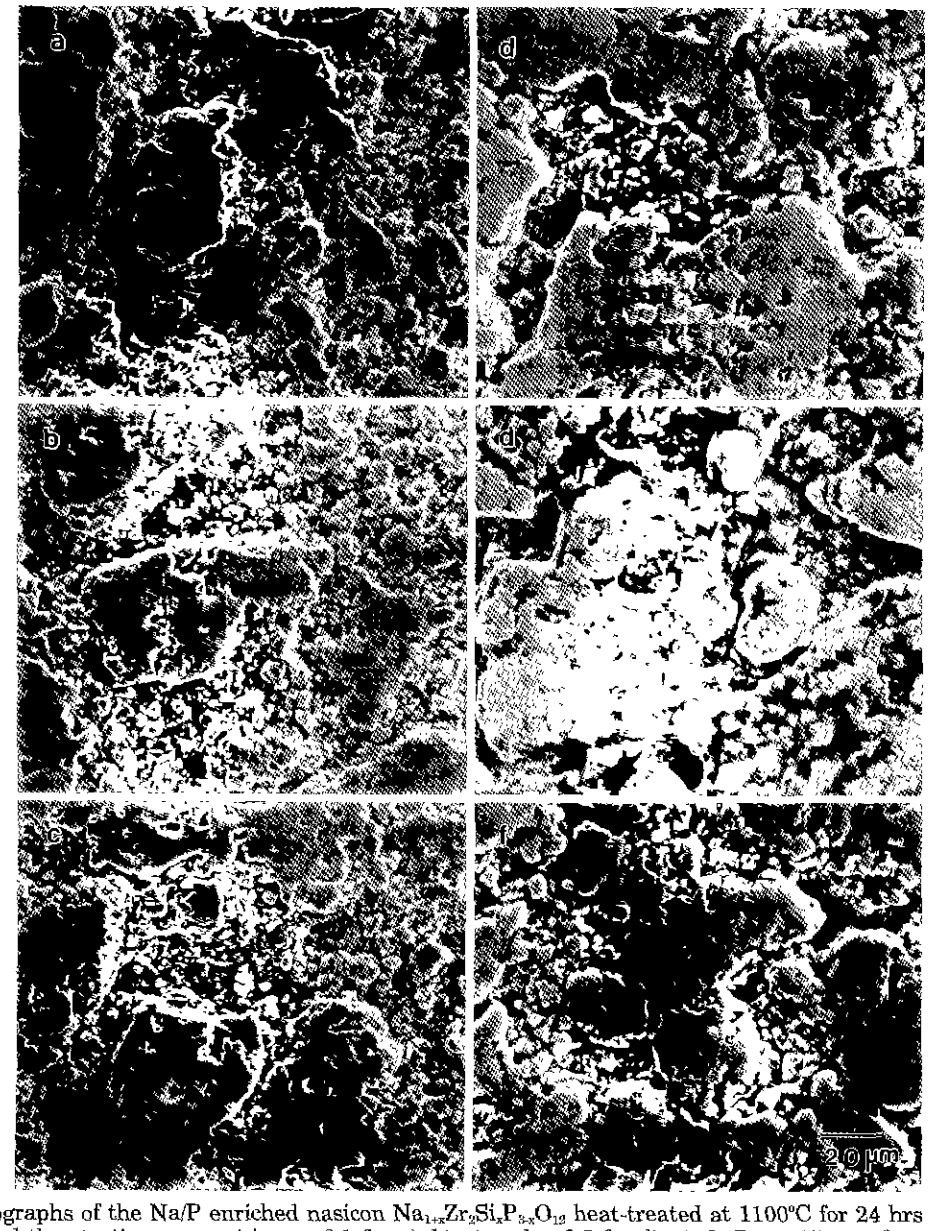

Fig. 6. SEM micrographs of the Na/P enriched nasicon $Na_{1+x}Zr_2Si_xP_{3-x}O_{12}$ heat-treated at 1100°C for 24 hrs with different oxygen partial pressure and the starting composition. x=2.1 for a), b), c) and x=2.2 for d), e), f). P_{O2}=0.15 atm for a) and d), 0.10 atm for b) and e), 0.05 atm for c) and f).

creasing the temperature to 1225 and 1250°C.

Although the formation of nasicon was accelerated and the reaction temperature decreased by adding excess Na and P to the starting composition, small amount of free ZrO_2 still existed in the sample.

4. Optimization of the heat-treatment variables

It was possible to synthesize the phase pure nasicon by XRD pattern without ZrO_2 peaks by optimizing the processing variables such as addition of 10 wt% of excess Na and P to the starting composition, heat treatment temperature of 1100~1150°C, repetition of heat treatments for 12 hrs, and the pulverizing and pelletizing procedure between the heat treatments. Next, several heat treatment profiles were tried to eliminate the glassy phase found at the grain boundaries of the nasicon (Fig. 9). The heat treatment profile was optimized to form the liquid phase in the initial stage of reaction and to secure a stable grain growth of nasicon in the later stage, which was conjectured from the microstructure of the sample after 1st and 2nd heat treatment. While maintaining the oxygen partial pressure at P_{O2}=0.1~0.15 atm, temperature was increased above the sintering temperature for a short time to accelerate the liquid formation, and annealing step below 1000°C was introduced after the reaction to avoid the formation of the glassy phase. Among various heat treatment profiles, nasicon without ZrO_2 and with minimized glassy phase was obtained by

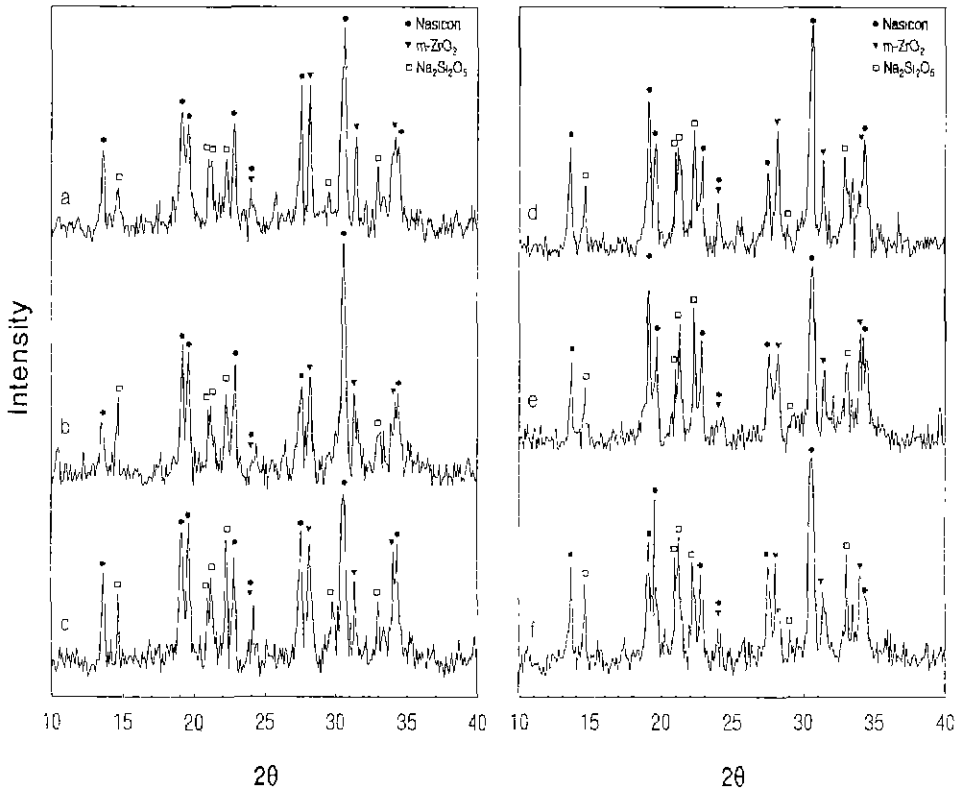

Fig. 7. XRD patterns of the $Na_{1+x}Zr_2Si_xP_{3-x}O_{12}$ with x=2.1 (a,b,c) and x=2.2 (d,e,f) after heat treatment at 1000°C, P_{O2}=0.05 atm (a, d), 0.10 atm (b,e), and 0.15 atm (c,f).

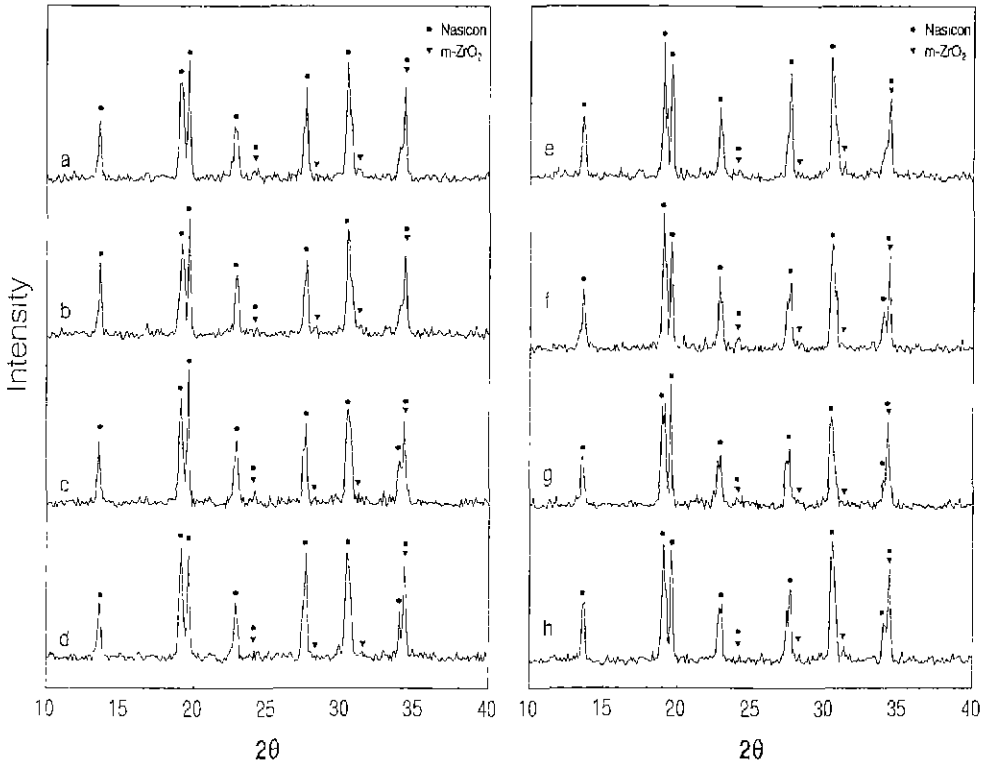

Fig. 8. XRD patterns of the Nasicon $Na_{1+x}Zr_2Si_xP_{3-x}O_{12}$ (x=2.1) covered with excess Na/P powder (a,b,c,d) and uncovered samples (e,f,g,h), which were heat-treated at 1100°C, P_{O_2}=0.05 atm (a,e), 0.10 atm (b,f), 0.15 atm (c,g), and 0.21 atm (d,h), respectively.

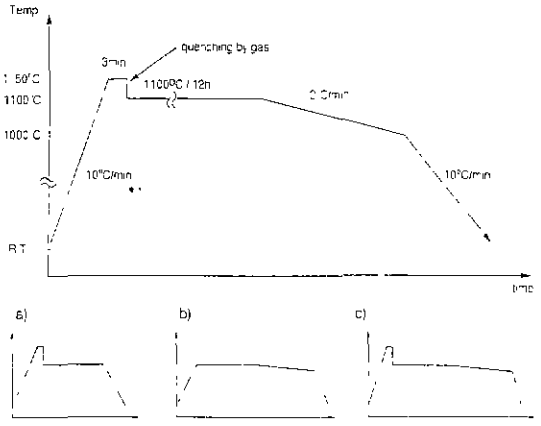

Fig. 9. Various heat-treatment profiles to reduce the ZrO_2 and glassy phase.

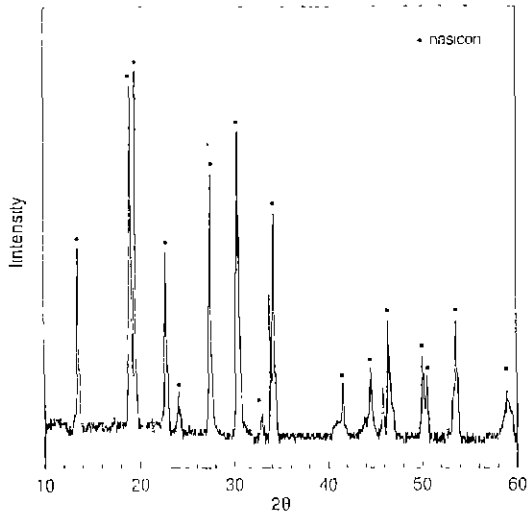

Fig. 10. XRD patterns of $Na_{1+x}Zr_2Si_xP_{3-x}O_{12}$ (x=2.1) with 10 wt.% excess Na and P. heat-treated by the profile in Fig. 9(c). The pattern shows only Nasicon phase and no ZrO_2 phase.

evacuating for 5 min at 1150°C, reacting at PO_2= 0.15 atm, T=1100°C for 12 hrs twice with intermittent grinding, and slow cooling after the reaction. The electrical conductivity from this sample showed a good electrical conductivity of $1\times10^{-2}(\Omega\cdot cm)^{-1}$ at 350°C, working temperature of high temperature battery.

IV. Conclusion

1) A solid state reaction process of nasicon for the mass production has been established which produce almost phase pure nasicon comparable the one obtained by sol-gel process by adding excess Na and P to the composition $Na_{1+x}Zr_2Si_xP_{3-x}O_{12}$ (x=2.1) and reacting at 1100~1150°C.

2) The volume fraction of ZrO_2 phase increased as with the heat treatment time due to the decomposition of nasicon.

3) The formation of nasicon was accelerated at oxygen partial pressure P_{O2}=0.1-0.15 atm and the volume fraction of glassy phase increased as P_{O2} decreased.

4) The optimized conditions for the synthesis of nasicon can be summarized as the composition $Na_{1+x}Zr_2Si_xP_{3-x}O_{12}$ (x= 2.1) with excess Na and P, reaction at T=1150°C and P_{O2}= 0.10~0.15 atm for 24 hrs, intermittent grinding between the heat treatments.

5) The electrical conductivity of the nasicon sample in this study showed a good electrical conductivity of ~1×10^{-2} $(\Omega\cdot cm)^{-1}$ at 350°C, working temperature of high temperature battery.

References

1. T. Takahashi, Superionic Solids and Solid Electrolytes, Recent Trends (ed. by A.L. Laskar and S. Chandra), 1-41, Academic Press, NY, (1989).
2 R. A. Huggins, Critical Materials Problems in Energy Production, ed. by Stein, Academic Press, (1976).
3 R. M. Dell, Electrode Processes in Solid State Ionics, ed. by M Kleitz and J. Dupuy, 389, D. Reidel Pub., (1976).
4. M. Voinov, *ibid.*, **431**, (1976).
5. H Y-P. Hong, "Crystal Structures and Crystal Chemistry in the System $Na_{1+x}Zr_2Si_xP_{3-x}O_{12}$," *Mat. Res. Bull.*, **11**, 173-182 (1976).
6. B. E. Yoldas and I. K. Lloyd, "Nasicon Formation by Chemical Polymerization," *Mat. Res. Bull.*, **18**, 1171-1177 (1983).
7. V. A. Nicholas, A. M. Heyns, A. I. Kimgon and J. B. Clark, "Reactions in the formation of $Na_5Zr_2Si_2PO_{12}$," *J. Mat. Sci.*, **21**, 1967-1973 (1986).
8. S. YDE-Anderson, J. S. Lundsgaard, L. Möller, and J. Engell, Solid State Ionics, **14**, 73-70 (1984).
9. U. Von Alpen, M. F. Bell. and H. H. Höfer, *Solid State Ionics*, **3/4**, 215-218 (1981).
10. J P. Boilet, G. Collin, and P. Colomban, "Relation Structure-fast Ion Conduction in the Nasicon Solid Solution," *J. Solid State Chem.*, **73**[1], 160-171 (1988).
11. R. S. Gordon, G. R. Miller, B. J. McEntire, E. D. Beck, and J R Rasmussen. "Fabricaion and Characterization of Nasicon Electrolytes," *Solid State Ionics*, **3/4**, 243-248 (1981).
12. K. D. Kreuer, H Kohler, and J. Maier, High Conductivity Solid Ionic Concuctors: Recent Trends and Applications, ed. by T. Takahashi, 242-279, World Scientific, (1989).
13. G. Collin and J P Boilet, Superionic Solids and Solid Electrolytes, Recent Trends, ed. by A. L. Laskar and S. Chandra, 227-263, Academic Press, NY, (1989).
14 H Perthuis and Ph. Colomban, "Well densified Nasicon type Ceramics, Elaborated using Sol-Gel Process and Sintering at Low Temperatures," *Mat. Res. Bull.*, **19**, 621-631 (1984).
15. R. S. Roth, ed., Phase Equilibria Diagrams, Vol. XI:Oxides, 11: 9740 (1995).